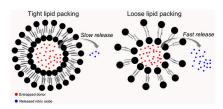# Controlled release of nitric oxide from liposomes

Dakota J. Suchyta, **Mark H. Schoenfisch**

Department of Chemistry, The University of North Carolina at Chapel Hill, 131 South Rd., Chapel Hill, North Carolina, 27599

Abstract

We report the ability to readily tune NO release from *N*-diazeniumdiolate-encapsulated liposomal structures by altering the NO donor molecule structure and/or phospholipid composition (independently or in combination). While encapsulating more stable NO donors expectedly enhanced the NO release (up to 48 h) from the liposomes, the phospholipid headgroup surface area proved equally useful in controlling NO-release kinetics by influencing the water uptake and concomitant *N*-diazeniumdiolate NO donor breakdown (to NO). The potential therapeutic utility of the NO-releasing liposomes was further assessed in biological/proteinaceous fluids. The NO-release kinetics were similar in buffer and serum.

Graphical Abstract

Keywords

Liposome; drug delivery; nitric oxide; controlled-release; serum; blood

Introduction

The drug delivery field has demonstrated that the encapsulation of therapeutics (e.g., antifungals, biocides, chemotherapeutics, and virucides) within liposomes is an effective strategy for controlled delivery to select targets of interest.[1–4] Using liposomes as drug delivery vehicles affords many benefits, including reduced immune response, increased cellular uptake, and protection of drug payload from premature action or breakdown.[5] Although liposomes passively localize themselves at the site of interest,[5] post-delivery

accumulation of the encapsulated therapeutic (e.g., cisplatin and doxorubicin) has been shown to negatively impact surrounding healthy tissue. [6–7] The need to develop therapeutics with limited off-target cytotoxicity remains highly desirable.

Nitric oxide (NO) is an endogenously produced free radical involved in multiple physiological processes, including blood pressure regulation, the immune response to pathogens, neurotransmission, and cellular proliferation.[8–11] Unlike current chemotherapeutics, NO is rapidly converted to a harmless metabolite (i.e., nitrite) and cleared in biological media, mitigating the toxic accumulation common to most drugs. Based on NO's promise as a potential therapeutic, a significant body of research has focused on strategies to exogenously deliver NO using synthetic NO donors, such as metal-NO complexes, S-nitrosothiols (RSNOs), and N-diazeniumdiolates.[12–16] N-diazeniumdiolates are a particularly attractive vehicle for NO storage and delivery because they undergo pH-dependent decomposition (faster release as the pH is lowered) to liberate NO (Scheme S1). Furthermore, the breakdown and release of NO is a direct function of the molecular structure of the donor, enabling exquisite control over the rate of release.[16] Structures bearing cationic primary amines can electrostatically stabilize their anionic diazeniumdiolate group, thus yielding longer NO-release half-lives. For example, spermine/NO (SPER/NO) exhibits a much longer half-life than proline/NO (PROLI/NO) at pH 7.4 ($t_{1/2}$ = 37 min and 2 s, respectively).[17] This breakdown of N-diazeniumdiolates to NO can be used therapeutically by exploiting the microenvironment of certain disease sites (e.g., cancer, dental caries, and ulcerative colitis) that exhibit a lowered pH due to altered cellular metabolisms. In contrast to healthy tissue where pH homeostasis is maintained near pH 7.4, these diseased tissues should promote more rapid NO release at the site of interest, thereby mitigating off-target cytotoxicity.[18–20]

Others have previously demonstrated that liposomes can encapsulate NO donors in order to enhance delivery and prolong NO release.[21–24] In contrast to these studies that used gaseous NO and NO photodonors, our lab has utilized encapsulated N-diazeniumdiolates to deliver NO. The liposomes exhibited enhanced NO donor stability (>3 mo shelf-life) along with greater *in vitro* cytotoxicity toward pancreatic cancer cells compared to the free, unencapsulated NO donor.[25] However, the kinetic tunability of this system was rather limited (i.e., controlled only by pH) with the relationship between liposomal characteristics (e.g., composition and size) and NO-release properties remaining unclear. As such, the focus of this research is developing strategies for altering the properties of NO release (e.g., half-life and total storage) by modifying the N-diazeniumdiolate and phospholipid structures. The utility of these changes on protein surface adsorption in serum (important to scaffold clearance from the bloodstream) is also investigated, with attention to NO-release properties as a function of solution media.[26–27]

Experimental Section

Materials.

Dimyristoylphosphatidylcholine (DMPC), dipalmitoylphosphatidylcholine (DPPC), distearoylphosphatidylcholine (DSPC), dipalmitoylphosphatidylglycerol (DPPG), dipalmitoyltrimethylammoniumpropane chloride salt (DPTAP),

dipalmitoylphosphatidylethanolamine-*N*-[methoxy(polyethyleneglycol)-2000] (DPPE-PEG2000), dipalmitoylphosphatidylethanolamine (DPPE), and distearoylphosphatidylethanolamine (DSPE) were purchased from Avanti Polar Lipids (Alabaster, AL). Cholesterol (Chol), *N*-propyl-1,3-propanediamine (PAPA), L-proline (PROLI), diethylamine (DEA), spermine (SPER), pyranine, coumarin, 5(6)-carboxyfluorscein, Dowex 1X2 chloride form (200-400 mesh) anion exchange resin, hemoglobin from bovine, and fetal bovine serum (FBS) were obtained from Sigma (St. Louis, MO). Chloroform, anhydrous acetonitrile, sulfuric acid, diethyl ether, sodium hydroxide, and the Bradford assay kit were purchased from Fisher Scientific (Fair Lawn, NJ). The source of Sephadex G-25 was GE Healthcare (Pittsburgh, PA). Pure nitric oxide (NO) gas (99.5%) was obtained from Praxair (Sanford, NC). Nitrogen (N_2), argon (Ar), and nitric oxide (NO) calibration gas cylinders (26.80 ppm, balance N_2) were obtained from Airgas National Welders (Durham, NC). A Millipore Milli-Q UV Gradient A10 System (Bedford, MA) was used to purify distilled water to a resistivity of 18.2 MΩ·cm and a total organic content of 6 ppb. Canine blood was freshly collected into EDTA-coated vacutainers by the Francis Owen Blood Lab (Carrboro, NC). Serum was isolated from the blood samples within 15 min of initial collection.

Synthesis of *N*-diazeniumdiolates.

A previously reported method was used to synthesize the NO donors.[17] Briefly, the precursor amine (i.e., PROLI, DEA, PAPA, or SPER) was dissolved in anhydrous acetonitrile at a concentration of 33.3 mg/mL. The solution was then purged with argon to 100 psi inside a stainless steel Parr bomb. Six sequential purges (three quick purges of 10 s each, followed by three slow purges of 10 min each) was used to remove residual oxygen. The solution was subsequently charged with 145 psi NO for 3 d. After 3 d, the solution was purged six times with argon to 100 psi to remove residual NO. The precipitated product was poured over a Hirsch funnel, washed twice with diethyl ether, and dried under vacuum overnight. The final NO-releasing product (i.e., PROLI/NO, DEA/NO, PAPA/NO, or SPER/NO) was stored at −20 °C until further use. Spectroscopic characterization was performed on the NO donors, including their decomposition products at pH 5.4 and 7.4 (Figures S1–S5).

Preparation and characterization of liposomes.

Liposomes were synthesized using a 1:1 molar ratio of lipid to Chol (49.5 μmol lipid:49.5 μmol Chol) following the report by Szoka and Papahadjopoulos.[28] Chloroform and diethyl ether (5 mL each) were used to dissolve the lipids in a round-bottomed flask under a N_2 atmosphere. The *N*-diazeniumdiolate donor (i.e., PROLI/NO, DEA/NO, PAPA/NO, or SPER/NO) was dissolved in 50 mM NaOH to make a 14 mM stock NO donor solution and subsequently injected (1.5 mL) into the flask, which was sonicated for 4 min at a temperature 5 °C higher than the transition temperature of the phospholipid. The organic phase was removed by rotoevaporation and the resulting liposomes incubated above their respective transition temperature for 30 min. The unencapsulated donor was removed using four Sephadex G-25 spin columns packed in 10-mL syringes. The final volume of purified liposomes collected from the column was stored at 4 °C. Fluorophore-encapsulated liposomes were prepared in the same manner as NO-releasing liposomes.

Characterization of liposome size.

Dynamic light scattering (DLS) measurements were performed to determine liposome size and polydispersity. The liposomes were diluted with water and their size characterized using a Zetasizer Nano (Malvern Instruments, UK). Transmission electron micrographs (TEM) were also collected to confirm liposome formation. Liposome samples for TEM analysis were prepared by diluting the stock solution with Milli-Q water (1:1 volumetric ratio) and casting the suspension onto Formvar-coated, square mesh copper TEM grids (Electron Microscopy Sciences, Hatfield, PA). The solvent was allowed to evaporate for 45 min prior to applying a negative-stain using 2% (w/v) uranyl acetate. A drop of the stain was left on the grid for 30 s after which the droplet was removed using filter paper. The sample was then allowed to dry for 5 min. The liposomes were imaged using a JEOL 100CX II transmission electron microscope at an accelerating voltage of 100 kV.

Nitric oxide release from liposomes.

Nitric oxide totals and the overall release kinetics were evaluated using a Sievers chemiluminescence Nitric Oxide Analyzer (NOA; Boulder, CO).[29–30] The instrument was calibrated using a NO zero filter (0 ppm NO) and a 26.80 ppm NO standard (balance N_2). An aliquot of the liposomes was injected into a 2:1 volumetric ratio of ethanol to 0.183 M sulfuric acid (30 mL total volume) at 37 °C to determine the NO donor encapsulation efficiency. The encapsulation efficiency, or the extent to which the NO donor is entrapped within the liposomal aqueous core, was calculated by comparing the liposome NO payload to the amount of NO in the free donor solution used during preparation of the liposomes. Studies to evaluate NO-release kinetics were performed in 10 mM MES buffer (pH 5.4) and 10 mM PBS (pH 7.4) at 37 °C. The presented data and error are from at least 3 separate liposome preparations. Nitric oxide release was terminated when the NO concentration dropped below 10 ppb per 300 μL liposomes.

Turbidity assay.

Liposomes (30 μL) were mixed with 600 μL FBS and incubated at 37 °C with slight agitation. After 1 h, 100 μL was removed, placed into a 96-well plate, and then the absorbance at 450 nm measured using a Thermoscientific Multiskan EX plate reader (Waltham, MA). The relative turbidity increase was compared against that of a control solution (30 μL of 50 mM NaOH mixed with 600 μL FBS). Of note, no further changes in turbidity were observed after 1 h incubation with FBS.

Serum protein adsorption to liposomes.

Quantification of proteins adsorbed to the liposome surface was measured using the Bradford assay.[31] Briefly, liposomes (20 μL) were mixed with 400 μL of a 10% (v/v in 10 mM PBS) FBS solution and incubated for 1 h at 37 °C with slight agitation. Afterwards, the liposomes were centrifuged (13,000 × g for 3 min) and washed twice with 10 mM PBS. The resulting lipid pellet was then dissolved in 100 μL of a 1:2 volumetric ratio of 10 mM PBS to ethanol. This dissolved pellet (30 μL) was added to a 96-well plate, mixed with 300 μL dye solution. After 10 min, the absorbance from the solution was measured at 595 nm.

Bovine serum albumin standards (330 μL total volume) were used to generate linear calibration curves.

Nitric oxide release from liposomes in whole blood and serum.

Nitric oxide release from liposomes was measured in both animal blood and serum. Briefly, liposomes (30 μL) were mixed with 600 μL freshly-obtained citrated whole blood or serum (pre-incubated at 37 °C). The solution was stored in a 37 °C incubator for a pre-determined period of time, after which an 80 μL aliquot was injected into a 2:1 volumetric ratio of ethanol to 0.183 M sulfuric acid (30 mL total volume) at 37 °C. The % NO remaining was determined by dividing the total NO released at each timepoint by the total NO released at the initial timepoint (~10 s after mixing liposomes with blood/serum) and multiplying by 100.

Results and Discussion

Nitric oxide donor structure.

An important aspect in choosing an appropriate delivery system is the ability to easily modify drug-release kinetics. Altering the release rates of most liposome systems requires varying the lipid bilayer composition (e.g., cholesterol content, phospholipid property). Such an approach is not ideal since other aspects of the scaffold (i.e., hydrophobicity, aggregation, and the potential immune response) will be inevitably altered as well. One unique advantage of *N*-diazeniumdiolate NO donors is the ability to independently manipulate liposomal NO-release kinetics at the molecular level using discrete NO donors. In this study, four different NO donors (Figure S6) were encapsulated within liposomes composed of DPPC.

The size, polydispersity, and encapsulation efficiency (EE) of each NO donor-containing liposome was measured to determine how varying the NO donor affected the resulting liposome (Table 1). As expected, sizes of the liposomes remained consistent (~200 nm) regardless of the encapsulated NO donor, likely the result of the donors' similar molecular weights. Low polydispersity index PDI values (~0.2) indicated that the liposomes were monodisperse and did not form aggregates. Both the size and monodispersity of the PAPA/NO liposomes were preserved even after a 3-month storage period at 4 °C (193 nm and 0.211, respectively). The average EE was approximately 35%, regardless of the NO donor, a value similar to reported values for other solutes encapsulated by reverse-phase evaporation methods.[24,28] The slightly lower EE observed for PROLI/NO liposomes (30%) is attributed to the unavoidable loss of NO during preparation. Indeed, this NO donor has a short NO-release half-life in its free form ($t_{1/2}= 2$ s).

Nitric oxide-release measurements.

Nitric oxide was measured in 10 mM PBS (pH 7.4, 37 °C) to evaluate the effect of NO donor identity on the liposomal NO-release rates under physiological conditions. Each of the encapsulated NO donors exhibited extended NO-release kinetics relative to the free NO donor (Table 2). For example, the half-life of SPER/NO increased from 37 min in its free form to ~2 d when encapsulated within the liposome. The prolonged NO release for all systems is attributed to the lipid bilayer providing a physical barrier against proton diffusion/

exchange into or with the aqueous core.[24] As the molar amount of the lipid was held constant for all liposomal preparations, the total NO payload was normalized to the volume of each liposome system injected during analysis. Relative to the average NO payloads reported previously for NO-releasing liposomes (~6 μmol NO/mL liposomes or ~0.25 μmol NO/mg lipid),[24] we measured payloads that were significantly larger (~8-9 μmol NO/mL) for DEA/NO, PAPA/NO, and SPER/NO containing liposomes. In contrast, the NO totals for the PROLI/NO liposomes were lower than other systems, which we again attributed to the rapid breakdown of the NO donor.

Nitric oxide release from the liposomes was also evaluated in 10 mM MES buffer (pH 5.4, 37 °C) to mimic NO release at more acidic disease sites (e.g., tumor microenvironments). A pH gradient is thus created across the lipid bilayer, causing a large influx of protons into the liposomal core that reduced the internal pH.[24] As expected, the lower intraliposomal pH resulted in rapid *N*-diazeniumdiolate decomposition, large levels of NO, and reduced NO-release half-lives for the four liposome systems (Table S1) relative to pH 7.4. The system with the most prolonged NO release (SPER/NO liposomes) exhibited a decrease in overall NO-release duration from >1 week (pH 7.4) to <48 h (pH 5.4). Dynamic light scattering measurements confirmed preservation of the liposome size (i.e., rupturing did not occur). Despite the significantly more rapid release, the NO-release kinetics were still tunable, even at low pH, with half-lives ranging from 4 min to 10 h depending on the *N*-diazeniumdiolate identity.

Effects of lipid bilayer hydrophobicity and charge.

The liposome structure and NO-release rates of PAPA/NO liposomes were studied as a function of the lipid bilayer composition and associated properties (lipid structures are provided in the Supporting Information). PAPA/NO was selected as the model NO donor for this work due to its moderate NO-release characteristics under the tested conditions. By preparing different liposomes using electrically neutral lipids of varying alkyl chain length (including DMPC, C_{14}, DPPC, C_{16}, and DSPC, C_{18}), liposome size and the NO-release characteristics could be studied as a function of bilayer hydrophobicity. In addition, parallel studies were performed using C_{16} cationic (DPTAP) and anionic (DPPG) lipids to investigate the effects of charge on these same properties. Charged lipids are typically used to encapsulate larger macromolecules (e.g., DNA) more effectively or to localize the vesicle at an area of interest due to coulombic attraction.[32–33] As the *N*-diazeniumdiolate NO donors are anionic, studying coulombic interactions using charged phospholipids, such as DPPG (negative) and DPTAP (positive), may elucidate unique effects on both EE and NO-release properties (i.e., NO payloads and release kinetics).

Varying the phospholipid's carbon chain length caused only slight deviations in the liposome size for the longest chain length (C_{18}), as indicated by DLS (Table 3) and TEM analysis (Figure S8). Liposomes made from DMPC (C_{14}) and DPPC (C_{16}) remained similar in size (~200 nm) with comparable PDI and EE values (~30%). In contrast, liposomes prepared using DSPC (C_{18}) were significantly larger (340 nm) and more polydisperse, likely due to the longer alkyl chains disrupting bilayer formation.[34] Anionic DPPG liposomes exhibited size and monodispersity similar to that of neutral DPPC liposomes (Table 3 and Figure S9),

but demonstrated an 11% decrease in EE. We hypothesize that the repulsive interactions between the negatively charged phospholipid and anionic *N*-diazeniumdiolate prevented efficient encapsulation within the liposomal core. The effects of coulombic charge were probed further by comparing the EE values of DPPC and DPPG liposomes encapsulating either neutral (coumarin) or negatively charged (carboxyfluorescein) fluorophores. While similar coumarin EE values were observed for both liposome systems, neutral DPPC liposomes exhibited greater encapsulation of carboxyfluorescein relative to anionic DPPG (Table S2). Therefore, charge interactions between the encapsulated molecule and the phospholipid may significantly affect the efficiency of drug encapsulation.

Liposomes prepared using cationic DPTAP lipids had comparable EE values to the neutral liposomes. However, DLS measurements revealed substantially larger and more polydisperse sizes relative to liposomes prepared using the other lipids (Table 3). Large PDI values have been previously reported for liposomes synthesized utilizing TAP-based lipids in high ionic strength solutions as a result of aggregation.[35–37] Indeed, we found that we were able to obtain better size (308 nm) and PDI values (0.316) after preparing DPTAP liposome solutions of a lower ionic strength (1 mM), corroborating the correlation between ionic strength and vesicle aggregation. As an alternative to changing the ionic strength, DPPC was employed as a co-lipid for DPTAP liposome preparation. Positively charged liposomes with a 50:50 DPPC:DPTAP molar ratio were characterized as having similar size, PDI, and EE (227 nm, 0.168, and 31%, respectively) compared to pure DPPC liposomes. By utilizing this method, cationic liposomes with sizes and PDI values mirroring those of neutral and anionic liposomal systems were readily achieved.

Bilayer properties and NO release.

Nitric oxide-release properties of the liposome systems were determined at pH 7.4 and 37 °C (Table 4). With the exception of the liposomes composed of negatively charged DPPG lipids, each liposome system studied exhibited similar NO payloads (~8.5 μmol/mL). Although the repulsive ionic forces lowered the NO totals of the DPPG liposomes, the release kinetics remained similar to that from neutral liposomes, indicating that bilayer water permeability was not appreciably influenced by the bilayer's negative charge. Conversely, aggregation of the positively charged DPTAP liposomes may likely have caused a greater proton influx to the liposome center with concomitantly more rapid NO release compared to the neutral liposome systems. To rule out the influence of electrostatically surface-bound NO donor on rapid NO release, DPTAP liposomes were incubated with an anion exchange resin. After filtering the liposomes from the resin, the measured NO-release kinetics were nearly identical to the liposomes prior to resin incubation, suggesting that DPTAP bilayer defects represent the only factor impacting the rapid NO release.

We initially hypothesized that the liposome NO-release kinetics would be prolonged as the hydrophobicity (i.e., carbon chain length) of the phospholipid was increased. While the C_{18}-containing DSPC liposomes exhibited significantly longer NO-release kinetics, the DMPC and DPPC systems demonstrated similar NO-release half-lives. As such, it seemed unlikely that the extended NO-release kinetics observed for the DSPC liposomes was a result of greater alkyl character or hydrophobicity. Further, differential release kinetics due to varying

transition phase temperatures between the phospholipids should not occur as cholesterol was included in all liposome formulations, which homogenizes the bilayer and attenuates the effects of temperature on ordering of the lipid phase.[38]

In lieu of hydrophobicity alone, the NO-release kinetics proved dependent on the compactness of the lipid chains upon liposome formation. Indeed, tighter packing of the lipid chains has been shown to occur as the headgroup surface area of the lipid decreases, resulting in reduced water permeability of the lipid bilayer.[39] Given the area per lipid headgroup being nearly identical for DMPC and DPPC ($\sim$0.655 nm^2) and distinct from DSPC ($\sim$0.430 nm^2),[40–41] the tighter lipid packing for the DSPC liposomes would slow the decrease in intraliposomal pH and *N*-diazeniumdiolate NO donor decomposition to NO.

Water permeation into the liposome core was characterized by examining intraliposomal pH changes using a fluorescent dye. Pyranine (10 μM), a bilayer-impermeable pH-sensitive dye, was encapsulated within the liposomes to probe internal pH changes over time. Under basic conditions, pyranine produces a strong fluorescent signal (λ = 520 nm) that reduces in intensity upon becoming protonated (i.e., as pH decreases).[42] After immersion into pH 7.4 buffer, the fluorescence from DMPC and DPPC liposomes would be expected to decrease at similar rates over time, whereas that from the DSPC liposomes would be more gradual due to the restricted water permeability. As shown in Figure 1, this behavior was followed exactly. Over 24 h, the fluorescence measured from DSPC liposomes approached that from the DMPC and DPPC vesicles. The smaller initial change in intraliposomal pH combined with the gradual fluorescence drop over time for DSPC liposomes clearly confirms the influence of headgroup-mediated water/proton permeation on NO release. Of note, DLS measurements confirmed typical size values, indicating that bursting of the liposomes did not occur during the experiment.

As shown in Figure 2, lipids with similar packing (i.e., headgroup surface area) exhibited nearly identical water/proton permeation with similar NO-release kinetics regardless of charge or headgroup moiety.[39] These results explain why the anionic (and lower EE) DPPG liposomes maintain identical NO-release properties as neutral DPPC liposomes. A range of NO-release kinetics is therefore possible by varying the lipid bilayer composition (both partially or completely). For example, we used a 10:90 DPPE:DPPC molar mixture to produce PAPA/NO liposomes with intermediate NO-release half-lives ($t_{1/2}$ = 3.7 h) relative to analogous single-lipid systems (DPPC $t_{1/2}$ = 2.5 h; DPPE $t_{1/2}$ = 6.6 h). Identical trends in NO release were observed at pH 5.4 (Table S3), indicating that the bilayer composition-mediated control over NO release was maintained at lower pH as well.

Nitric oxide-release kinetics in biological media.

Bilayer composition has been shown to influence the *in vivo* fate of liposomes.[46] For example, cationic liposomes are efficiently uptaken or internalized by cells, attributed to the electrostatic interactions with negatively charged cell membranes.[47] Charged liposomes also promote protein binding and opsonization, facilitating rapid clearance from the bloodstream. [48] We thus investigated if the liposomal surface properties (e.g., charge and PEGylation) affected the NO-release kinetics in biological fluids where protein adsorption may occur. DPPC (neutral), DPPG (negative), 50:50 DPTAP:DPPC (positive), and 10:90 DPPE-PEG/

DPPC (PEGylated) liposomes were selected due to their similar NO release ($t_{1/2}$ ~2.5 h) and long-term structural stability (Figure S10).

NO-release kinetics were first measured in serum to determine if permanent or transient defects form in the liposome bilayer upon protein fouling, perhaps altering the NO release. Surprisingly, the NO release did not change appreciably (Figure 4a). Indeed, the liposomes exhibited similar half-lives ($t_{1/2}$ ~2.5 h) to those measured in PBS, which agrees with the minimal protein adsorption that had occurred on the liposome surface in serum (Figures S11).[49–52]

While measuring NO release in serum elucidated the effects of proteins on liposomal NO-release kinetics, serum lacks a number of complex cellular components and molecules (e.g., hemoglobin) that are capable of scavenging NO. Nevertheless, nearly analogous NO release was measured in whole blood between the different liposome compositions (Figure 4b). Even the PEG-stabilized liposomes exhibited only slight initial differences in NO-release rates. These results indicate that the surface properties of PAPA/NO-containing liposomes (e.g., charge) can be controlled independently of NO-release kinetics in blood, to achieve potential targeting and/or adjusting bloodstream clearance.

A notable decrease in the NO-release half-life in blood was observed relative to PBS and serum. For example, neutral DPPC PAPA/NO liposomes having similar PBS and serum NO release ($t_{1/2}$ = 2.6 ± 0.4 and 2.9 ± 1.0 h, respectively), exhibited 60% faster NO release ($t_{1/2}$ = 1.0 ± 0.2 h) in whole blood (Figure 5). We hypothesize that these results are caused by the high concentration of NO scavengers in blood.[53] At concentrations from 129–177 mg/mL (12.9–17.7 g/dL) in humans, hemoglobin is among the most active NO scavengers in the bloodstream due to iron-NO radical complexation.[53–58] As such, scavenging would lead to an increase in the measured real time NO-release kinetics due to the consumption of detectable NO. To explore this, NO release from neutral DPPC PAPA/NO liposomes was measured in 10 mM PBS (pH 7.4, 37 °C) containing 157 mg/mL hemoglobin (Figure S12). The measured NO-release half-life indeed decreased ($t_{1/2}$ = 0.5 h) relative to in pure PBS ($t_{1/2}$ = 2.6 h), supporting blood hemoglobin being at least partially responsible for the observed differences in the NO-release kinetics for blood versus PBS/serum. The disparity between blood and PBS containing hemoglobin is likely due to compartmentalization of hemoglobin within erythrocytes (not free, as in the PBS solution), leading to less overall NO scavenging and longer measured NO-release durations.[54] Of note, negligible hemolytic activity of the NO-releasing liposome systems (Figure S13) indicates that the liposomes do not enhance liberation of intracellular hemoglobin.

Conclusions

Herein, the ability to precisley control NO-release half-lives was demonstrated by selection of an appropiate NO donor and varying the composition of the lipid bilayer. We found that the lipid headgroup surface area was the defining factor that controlled NO-release kinetics due to the dependence of bilayer proton permeability on lipid packing density. Liposomes prepared using different ionic charges and PEG-modified lipids exhibited low protein adsorption (5 g protein/mol lipid) and similar NO release in PBS and serum, regardless of

the lipid identity. However, the overall NO-release flux in whole blood compared to PBS and serum was less, and thus the NO-release kinetics appeared shorter. These results were attributed to the large concentrations of hemoglobin in blood, a known NO scavenger. Our study may provide guidance for the development of other macromolecular scaffolds with respect to how charge may affect protein adsorption and the influence of complex cellular components of blood on *in vivo* NO-release kinetics.

Supplementary Material

Refer to Web version on PubMed Central for supplementary material.

ACKNOWLEDGMENTS

REFERENCES

(1). Lopez-Berestein G Liposomes as carriers of antifungal drugs. Ann. New York Acad. Sci 1988, 544, 590–597. [PubMed: 3214094]

(2). Jones MN Use of liposomes to deliver bactericides to bacterial biofilms. Methods Enzymol. 2005, 391, 211–228. [PubMed: 15721384]

(3). Lammers T; Kiessling F; Hennink WE; Storm G Drug targeting to tumors: Principles, pitfalls, and (pre-) clinical progress. J. Control. Release, 2012, 161, 175–187. [PubMed: 21945285]

(4). Wutzler P; Sauerbrei A; Klöcking R; Brögman B; Reimer K Virucidal activity and cytotoxicity of the liposomal formulation of povidone-iodine. Antiviral Res. 2002, 54, 89–97. [PubMed: 12062394]

(5). Torchilin VP Recent advances with liposomes as pharmaceutical carriers. Nat. Rev. Drug Discov 2005, 4, 145–160. [PubMed: 15688077]

(6). De Angelis A; Urbanek K; Cappetta D; Piegari E; Ciuffreda L; Rivellino A; Russo R; Esposito G; Rossi F; Berrino L Doxorubicin cardiotoxicity and target cells: A broader perspective. Cardio-Oncol. 2016, 2, 1–8.

(7). Galluzzi L; Vitale I; Michels J; Brenner C; Szabadkai G; Harel-Bellan A; Castedo M; Kroemer G Systems biology of cisplatin resistance: Past, present, and future. Cell Death Dis. 2014, 5, 1–18.

(8). Moncada S; Palmer R; Higgs E Nitric oxide: Physiology, pathophysiology, and pharmacology. Pharmacol. Rev 1991, 43, 109–142. [PubMed: 1852778]

(9). Thomas DD; Ridnour LA; Isenberg JS; Flores-Santana W; Switzer CH; Donzelli S; Hussain P; Vecoli C; Paolocci N; Ambs S; Colton CA; Harris CC; Roberts DD; Wink DA The chemical biology of nitric oxide: Implications in cellular signaling. Free Radical Biol. Med 2008, 45, 18–31. [PubMed: 18439435]

(10). Gross SS; Wolin MS; Nitric oxide: Pathophysiological mechanisms. Annu. Rev. Physiol 1995, 57, 737–769. [PubMed: 7539995]

(11). Rosselli M; Keller PJ; Dubey RK Role of nitric oxide in the biology, physiology, and pathophysiology of reproduction. Hum. Reprod. Update, 1998, 4, 3–24. [PubMed: 9622410]

(12). Carpenter AW; Schoenfisch MH Nitric oxide release: part II. Therapeutic applications. Chem. Soc. Rev 2012, 41, 3742–3752. [PubMed: 22362384]

(13). Nichols SP; Storm WL; Koh A; Schoenfisch MH Local delivery of nitric oxide: targeted delivery of therapeutics to bone and connective tissues. Adv. Drug Deliv. Rev 2012, 64, 1177–1188. [PubMed: 22433782]

(14). Huerta S; Chilka S; Bonavida B Nitric oxide donors: novel cancer therapeutic (review). Int. J. Oncol 2008, 33, 909–927. [PubMed: 18949354]

(15). Wang PG; Xian M; Tang X; Wu X; Wen Z; Cai T; Janczuk AJ Nitric oxide donors: Chemical activities and biological applications. Chem. Rev 2002, 102, 1091–1134. [PubMed: 11942788]

(16). Hrabie JA; Keefer LK Chemistry of the nitric oxide-releasing diazeniumdiolate ("nitrosohydroxylamine") functional group and its oxygen-substituted derivatives. Chem. Rev 2002, 102, 1135–1154. [PubMed: 11942789]

(17). Hrabie JA; Klose JR; Wink DA; Keefer LK New nitric oxide-releasing zwitterions derived from polyamines. J. Org. Chem 1993, 58, 1472–1476.

(18). Tannock IF; Rotin D Acid pH in tumors and its potential for therapeutic exploitation. Cancer Res. 1989, 49, 4373–4384. [PubMed: 2545340]

(19). Loesche WJ Role of *streptococcus mutans* in human dental decay. Microbiol. Rev 1986, 50, 353–380. [PubMed: 3540569]

(20). Fallingborg J; Christensen A; Jacobsen B; Rasmussen S Very low intraluminal colonic pH in patients with active ulcerative colitis. Digest. Dis. Sci 1993, 38, 1989–1993. [PubMed: 8223071]

(21). Ostrowski AD; Lin BF; Tirrell MV; Ford PC Liposome encapsulation of a photochemical NO precursor for controlled nitric oxide release and simultaneous fluorescence imaging. Molec. Pharm 2012, 9, 2950–2955. [PubMed: 22953784]

(22). Giancane G; Valli L; Sortino S Dual-function multilayers for the photodelivery of nitric oxide and singlet oxygen. ChemPhysChem. 2009, 10, 3077–3082. [PubMed: 19816892]

(23). Huang S; Kee PH; Kim H; Moody MR; Chrzanowski SM; MacDonald RC; McPherson DD Nitric oxide loaded echogenic liposomes for nitric oxide delivery and inhibition of intimal hyperplasia. J. Am. Coll. Cardiol 2009, 54, 652–659. [PubMed: 19660697]

(24). Klegerman ME; Wassler M; Huang S; Zou Y; Kim H; Shelat HS; Holland CK; Geng Y; McPherson DD Liposomal modular complexes for simultaneous targeted delivery of bioactive gases and therapeutics. J. Control. Release, 2010, 142, 326–331. [PubMed: 19903503]

(25). Suchyta DJ; Schoenfisch MH Encapsulation of *N*-diazeniumdiolates within liposomes for enhanced nitric oxide donor stability and delivery. Mol. Pharm 2015, 12, 3569–3574. [PubMed: 26287799]

(26). Mahon E; Salvati A; Bombelli FB; Lynch I; Dawson KA Designing the nanoparticle-biomolecule interface for "targeting and therapeutic delivery". J. Control. Release, 2012, 161, 164–174. [PubMed: 22516097]

(27). Göppert TM; Müller RH Adsorption kinetics of plasma proteins on solid lipid nanoparticles for drug targeting. Int. J. Pharm 2005, 302, 172–186. [PubMed: 16098695]

(28). Szoka F Jr.; Papahadjopoulos D Procedure for preparation of liposomes with large internal aqueous space and high capture by reverse-phase evaporation. Proc. Natl. Acad. Sci 1978, 75, 4194–4198. [PubMed: 279908]

(29). Soto RJ; Yang L; Schoenfisch MH Functionalized mesoporous silica via an aminosilane surfactant ion exchange reaction: Controlled scaffold design and nitric oxide release. ACS Appl. Mater. Interfaces, 2016, 8, 2220–2231. [PubMed: 26717238]

(30). Worley BV; Schilly KM; Schoenfisch MH Anti-biofilm efficacy of dual-action nitric oxide-releasing alkyl chain modified poly(amidoamine) dendrimers. Mol. Pharm 2015, 12, 1573–1583. [PubMed: 25873449]

(31). Bradford MM A rapid and sensitive method for the quantitation of microgram quantities of protein utilizing the principle of protein-dye binding. Anal. Biochem 1976, 72, 248–254. [PubMed: 942051]

(32). Felgner PL; Gadek TR; Holm M; Roman R; Chan HW; Wenz M; Northrop JP; Ringold GM; Danielsen M Lipofection: A highly efficient, lipid-mediated DNA-transfection procedure. Proc. Natl. Acad. Sci 1987, 84, 7413–7417. [PubMed: 2823261]

(33). Campbell RB; Fukumura D; Brown EB Cationic charge determines the distribution of liposomes between the vascular and extravascular compartments of tumors. Cancer Res. 2002, 62, 6831–6836. [PubMed: 12460895]

(34). Nyren-Erickson EK; Haldar MK; Totzauer JR; Ceglowski R; Patel DS; Friesner DL; Srivastava DK; Mallik S Glycosaminoglycan-mediated selective changes in the aggregation states, zeta

potentials, and intrinsic stability of liposomes. Langmuir, 2012, 28, 16115–16125. [PubMed: 23102026]

(35). Wieber A; Selzer T; Kreuter J Physico-chemical characterisation of cationic DOTAP liposomes as drug delivery system for a hydrophilic decapeptide before and after freeze-drying. Eur. J. Pharm. Biopharm 2012, 80, 358–367. [PubMed: 22119734]

(36). Tavakoli S; Tamaddon A; Golkar N; Samani S Microencapsulation of (deoxythymidine)$_{20}$-DOTAP complexes in stealth liposomes optimized by Taguchi design. J. Liposomes Res 2015, 25, 67–77.

(37). Wasan EK; Harvie P; Edwards K; Karlsson G; Bally MB A multi-step lipid mixing assay to model structural changes in cationic lipoplexes used for in vitro transfection. Biochim. Biophys. Acta, 1999, 1461, 27–46. [PubMed: 10556486]

(38). Redondo-Morata L; Giannotti ML; Sanz F Influence of cholesterol on the phase transition of lipid bilayers: A temperature-controlled force spectroscopy study. Langmuir, 2012, 28, 12851–12860. [PubMed: 22873775]

(39). Mathai JC; Tristram-Nagle S; Nagle JF; Zeidel ML Structural determinants of water permeability through the lipid membrane. J. Gen. Physiol 2008, 131, 69–76. [PubMed: 18166626]

(40). Magarkar A; Dhawan V; Kallinteri P; Viitala T; Elmowafy M; Róg T; Bunker A Cholesterol level affects surface charge of lipid membranes in saline solution. Sci. Rep 2014, 21, 5005.

(41). Kupiainen M; Falck E; Ollila S; Niemelä P; Gurtovenko A Free volume properties of sphingomyelin, DMPC, DPPC, and PLPC bilayers. J. Comput. Thero. Nanos 2005, 2, 401–413.

(42). Clement NR; Gould JM Pyranine (8-hydroxy-1,3,6-pyrenetrisulfonate) as a probe of internal aqueous hydrogen ion concentration in phospholipid vesicles. Biochemistry, 1981, 20, 1534–1538. [PubMed: 6261798]

(43). Bensikaddour H; Snoussi K; Lins L; Bambeke F; Tulkens PM; Brasseru R; Goormaghtigh E; Mingeot-Leclercq M Interaction of ciprofloxacin with DPPC and DPPG: Fluorescence anisotropy, ATR-FTIR and ^{31}P NMR spectroscopies and conformational analysis. Biochim. Biophys. Acta, 2008, 1778, 2535–2543. [PubMed: 18809375]

(44). Leekumjorn S; Sum AK Molecular simulation study of structural and dynamic properties of mixed DPPC/DPPE bilayers. Biophys. J 2006, 90, 3951–3965. [PubMed: 16533838]

(45). Kuhl TL; Majewski J; Wong JY; Steinberg S; Leckband DE; Israelachvili JN; Smith GS A neutron reflectivity study of polymer-modified phospholipid monolayers at the solid-solution interface: Polyethylene glycol-lipids on the silane-modified substrates. Biophys. J 1998, 75, 2352–2362. [PubMed: 9788930]

(46). Pattni BS; Chupin VV; Torchilin VP New developments in liposomal drug delivery. Chem. Rev 2015, 115, 10938–10966. [PubMed: 26010257]

(47). Campbell RB; Fukumura D; Brown EB; Mazzola LM; Izumi Y; Jain RK; Torchilin VP; Munn LL Cationic charge determines the distribution of liposomes between the vascular and extravascular compartments of tumors. Cancer Res. 2002, 62, 6831–6836. [PubMed: 12460895]

(48). Gregoriadis G Overview of liposomes. J. Antimicrob. Chemother 1991, 28, 39–48.

(49). Oku N; Tokudome Y; Namba Y; Saito N; Endo M; Hasegawa Y; Kawai M; Tsukada H; Okada S Effect of serum protein binding on real-time trafficking of liposomes with different charges analyzed by positron emission tomography. Biochim. Biophys. Acta, 1996, 1280, 149–154. [PubMed: 8634309]

(50). Price ME; Cornelius RM; Brash JL Protein adsorption to polyethylene glycol modified liposomes from fibrinogen solution and from plasma. Biochim. Biophys. Acta, 2001, 1512, 191–205. [PubMed: 11406096]

(51). Kuznetsova RR; Vodovozova EL Differential binding of plasma proteins by liposomes loaded with lipophilic prodrugs of methotrexate and melphalan in the bilayer. Biochemistry (Mosc.), 2014, 79, 797–804. [PubMed: 25365489]

(52). Chonn A; Semple SC; Cullis PR Association of blood proteins with large unilamellar liposomes *in vivo*. J. Biol. Chem 1992, 267, 18759–18765. [PubMed: 1527006]

(53). Butler AR; Megson IL; Wright PG Diffusion of nitric oxide and scavenging by blood in the vasculature. Biochim. Biophys. Acta, 1998, 1425, 168–176. [PubMed: 9813307]

(54). Azarov I; Huang KT; Basu S; Gladwin MT; Hogg N; Kim-Shapiro DB Nitric oxide scavenging by red blood cells as a function of hematocrit and oxygenation. J. Biol. Chem 2005, 280, 39024–39032. [PubMed: 16186121]

(55). Kim-Shapiro DB; Schechter AN; Gladwin MT Unraveling the reactions of nitric oxide, nitrite, and hemoglobin in physiology and therapeutics. Arterioscler. Thromb. Vasc. Biol 2006, 26, 697–705. [PubMed: 16424350]

(56). Van Slyke DD; Philips RA; Dole VP; Hamilton PB; Archibald RM; Plazin J Calculation of hemoglobin from blood specific gravities. J. Biol. Chem 1950, 183, 349–360.

(57). Beutler E; Waalen J The definition of anemia: What *is* the lower limit of normal of the blood hemoglobin concentration. Blood, 2006, 107, 1747–1750. [PubMed: 16189263]

(58). Hunter RA; Storm WL; Coneski PN; Schoenfisch MH Inaccuracies of nitric oxide measurement methods in biological media. Anal. Chem 2013, 85, 1957–1963. [PubMed: 23286383]
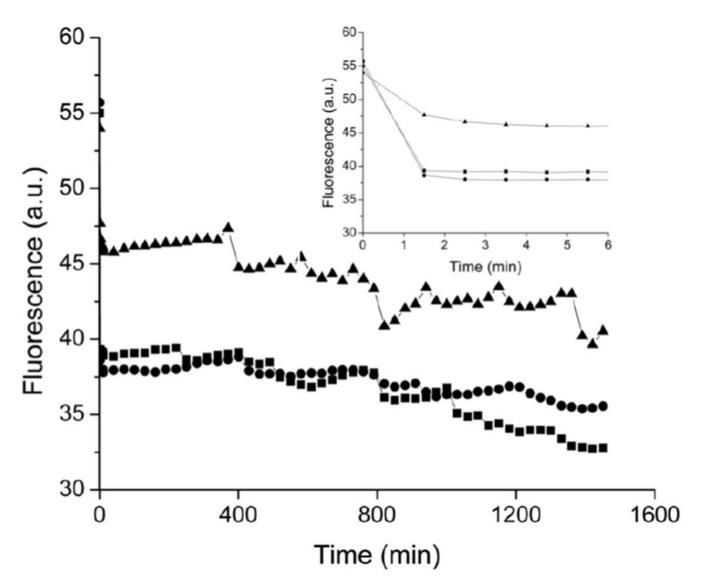
Figure 1.
Fluorescence emission at 520 nm from pyranine-encapsulated (■) DMPC, (●) DPPC, and
(▲) DSPC liposomes diluted 100-fold in 10 mM PBS (pH 7.4, 37 °C) as a function of time.
The spectra were collected using a 450 nm excitation wavelength. Inset depicts fluorescence
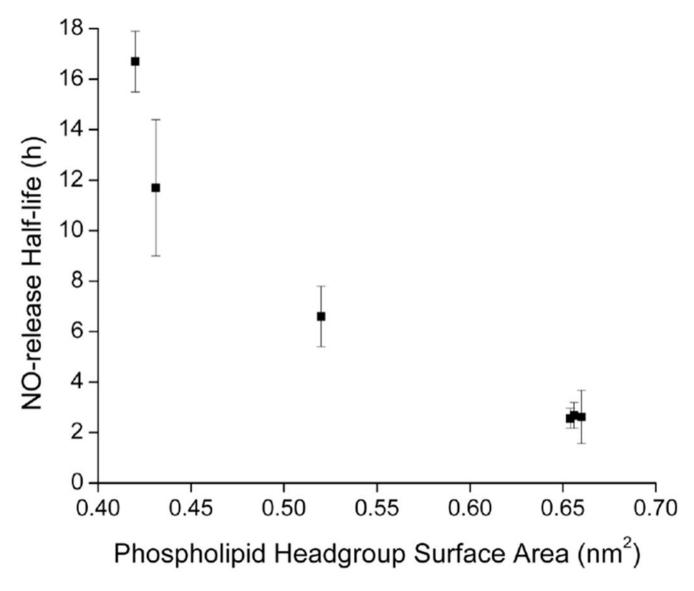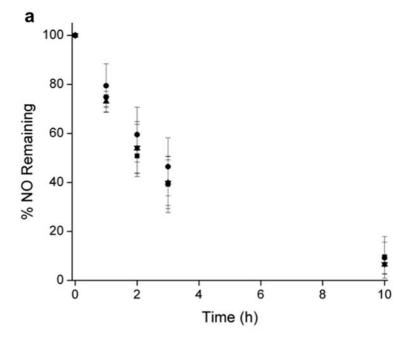from the first 5 min of data collection.

Figure 2.
Relationship between the liposomal NO-release half-life and phospholipid headgroup
surface area using PAPA/NO-encapsulated liposomes. Each point represents a different
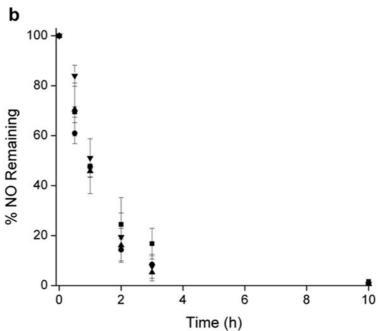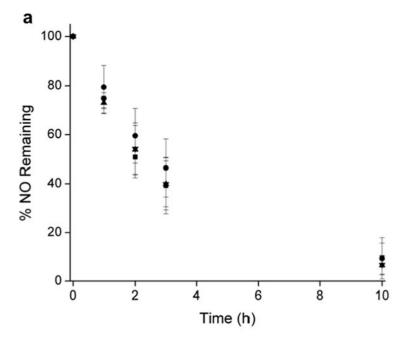phospholipid (see Materials section for list of lipids).[40–41,43–45]

Figure 3.
Nitric oxide release in (a) serum and (b) blood from (■) neutral DPPC, (▲) anionic DPPG, (●) cationic DPTAP, and (▼) PEGylated PAPA/NO liposomes.
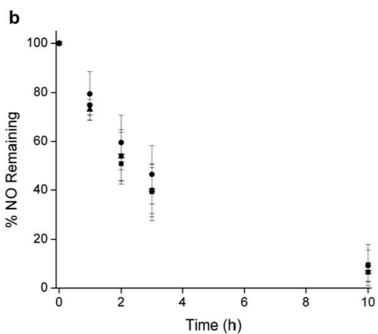
Figure 4.
Nitric oxide release in (a) serum and (b) blood from (■) neutral DPPC, (▲) anionic DPPG, (●) cationic DPTAP, and (▼) PEGylated PAPA/NO liposomes.
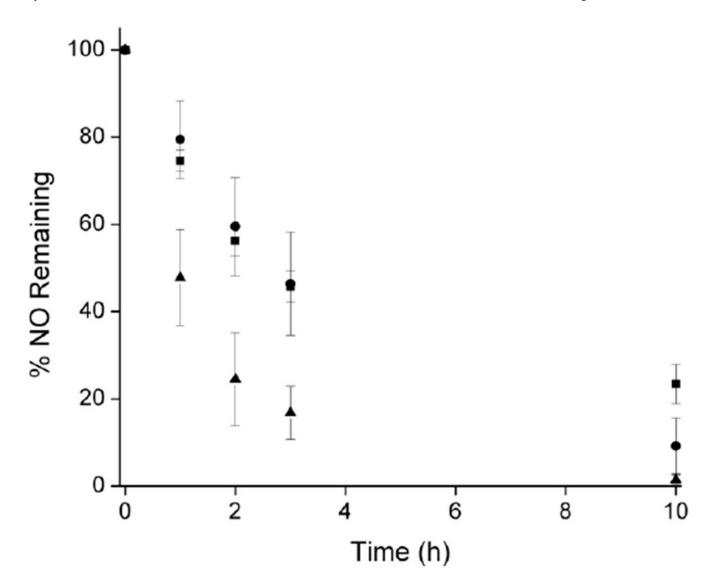
Figure 5.
Neutral DPPC PAPA/NO liposome NO-release kinetics in (■) PBS, (●) serum, and (▲) blood. Statistical analysis yielded $p < 0.02$ between all PBS and blood values.

Table 1.

Physicochemical properties of DPPC liposomes encapsulating various NO donors.

NO donor	Size ^{a} (nm)	Polydispersity index	Encapsulation efficiency ^{b} (%)
PROLI/NO	174 ± 18	0.166 ± 0.018	30.6 ± 1.9
DEA/NO	234 ± 20	0.185 ± 0.024	33.7 ± 4.2
PAPA/NO	203 ± 33	0.167 ± 0.070	33.4 ± 3.1
SPER/NO	248 ± 54	0.251 ± 0.020	38.3 ± 3.9

^{a}Z-average size measured using DLS.

^{b}Ratio of μmol of NO inside liposomes to μmol used for synthesis multiplied by 100.

Table 2.

Nitric oxide-release properties of DPPC liposomes as a function of NO donor in PBS (pH 7.4) at 37 °C.

NO donor	$t_{1/2}$ [a] (h)	t_d [b] (h)	$[NO]_{total}$ [c] (µmol/mL)
PROLI/NO	0.16 ± 0.05	2.8 ± 0.1	5.10 ± 0.51
DEA/NO	0.31 ± 0.02	4.6 ± 2.3	9.16 ± 0.33
PAPA/NO	2.6 ± 0.4	43.4 ± 3.9	8.83 ± 0.64
SPER/NO	45.3 ± 4.6	168.2 ± 17.0	7.73 ± 0.71

[a] Half-life of NO release.

[b] Duration of NO release.

[c] Total amount of NO released normalized to the injected volume from the liposome stock solution. Respective pH 7.4 half-lives of free (i.e., unencapsulated) PROLI/NO, DEA/NO, PAPA/NO, SPER/NO at 37 °C : 2 s, 2 min, 15 min, and 37 min.

Table 3.

Physicochemical properties of PAPA/NO liposomes as a function of bilayer composition.

Lipid [a]	Size [b] (nm)	Polydispersity index	Encapsulation efficiency [c] (%)
DMPC (C_{14})	236 ± 44	0.215 ± 0.050	30.3 ± 1.5
DPPC (C_{16})	203 ± 33	0.167 ± 0.070	33.4 ± 3.1
DSPC (C_{18})	340 ± 77	0.328 ± 0.080	32.2 ± 2.7
DPPG ($- C_{16}$)	161 ± 11	0.203 ± 0.030	22.0 ± 3.2
DPTAP ($+ C_{16}$)	446 ± 63	0.497 ± 0.120	29.4 ± 0.6

[a] Charge and alkyl chain length of the lipid is denoted in parentheses.

[b] Z-average size measured using DLS.

[c] Ratio of the μmol of NO inside the liposomes to the μmol used for the synthesis, multiplied by 100.

Table 4.

Nitric oxide-release properties of PAPA/NO liposomes as a function of bilayer hydrophobicity and charge in PBS (pH 7.4) at 37 °C.

Lipid	$t_{1/2}$[a] (h)	t_d[b] (h)	$[NO]_{total}$[c] (µmol/mL)
DMPC (C$_{14}$)	2.6 ± 0.5	42.9 ± 5.1	8.26 ± 0.29
DPPC (C$_{16}$)	2.6 ± 0.4	43.4 ± 3.9	8.83 ± 0.64
DSPC (C$_{18}$)	16.7 ± 1.2	85.6 ± 7.6	9.00 ± 0.74
DPPG ($-$ C$_{16}$)	2.6 ± 1.0	38.1 ± 1.8	6.33 ± 1.17
DPTAP ($+$ C$_{16}$)	0.9 ± 0.4	18.4 ± 1.9	8.63 ± 0.43

[a]Half-life of NO release.

[b]Duration of NO release.

[c]Total amount of NO released normalized to the injected volume from the liposome stock solution.